ANALYSIS OF THE INORGANIC CONSTITUENTS IN LOW-RANK COALS

G. P. Huffman and F. E. Huggins

U.S. Steel Corporation, Research Laboratory
125 Jamison Lane, Monroeville, PA 15146

Introduction

In recent years, numerous modern analytical techniques have been applied to the analysis of the inorganic constituents in coal. At the U.S. Steel Research Laboratory, Mossbauer spectroscopy and computer-controlled scanning electron microscopy have been emphasized(1-5). With the advent of very intense synchrotron radiation sources, the technique of extended X-ray absorption fine structure (EXAFS) spectroscopy has been applied in many areas of materials science, and several very recent articles on EXAFS studies of the inorganic constituents of coal have appeared(6-8). For the most part, previously published work has reported investigations of bituminous coals by these three techniques. In the current article, we present some examples of the analysis of the inorganic constituents of lower-rank coals, principally lignites, by these methods. Although the suite of low-rank coals investigated is rather limited, some distinct differences between the inorganic phase distributions in these coals and those in bituminous coals are apparent.

Experimental

Mossbauer spectroscopy is a spectroscopy based on the resonant emission and absorption of low-energy nuclear gamma rays. The ^{57}Fe nucleus exhibits the best Mossbauer properties of all isotopes for which the Mossbauer effect has been observed, and ^{57}Fe Mossbauer spectroscopy is perhaps the best method available for quantitative analysis of the iron-bearing phases in complex, multiphase samples. As discussed in recent review articles(2,9,10) every iron-bearing compound exhibits a characteristic Mossbauer absorption spectrum, and the percentage of the total iron contained in each phase can be determined from absorption peak areas. Detailed descriptions of the Mossbauer spectrometer and data analysis programs used in this laboratory, and discussion of the physical basis of the Mossbauer technique are given elsewhere(10).

The computer-controlled scanning electron microscope (CCSEM) developed in this laboratory consists of an SEM interfaced by minicomputer to a beam-control unit and an energy dispersive X-ray analysis system. Detailed descriptions of this instrument and its use in the determination of coal mineralogy and other applications are given elsewhere(3,11). Briefly, the beam is stepped across the sample in a coarse grid pattern, with typically 300 x 300 grid points covering the field of view. At each point, the backscattered electron intensity is sampled, and the minicomputer decides whether or not the beam is on a particle. Once a particle is identified, the grid density is increased to 2048 x 2048 and the area of the particle is measured. The beam-control unit then places the electron beam back

at the center of the particle and an energy dispersive X-ray spectrum is collected. Each particle is then placed into one of up to 30 categories (minerals, compounds, etc.) on the basis of the chemistry indicated by its X-ray emission spectrum, and approximate weight percentages of all categories are calculated. CCSEM is capable of measuring the size and chemical composition of up to 1000 particles per hour for many kinds of particulate samples.

EXAFS spectroscopy examines the oscillatory fine structure above the absorption edge in the X-ray absorption spectrum of a particular element. These oscillations arise from interference between the outgoing photoelectron wave and scattered waves produced by interaction of the photoelectrons with neighboring atoms. As discussed elsewhere (12,13), Fourier transform techniques can be used to extract from these oscillations information about the bond distances, coordination numbers, and types of ligands surrounding the absorbing element. Additional information about the valence or electronic state of the absorbing ion and the ligand symmetry can be obtained from examining the X-ray absorption near-edge spectra, or XANES, in the energy region very close to the absorption edge (within approximately $\pm$20-30 eV). Such XANES spectra frequently provide characteristic fingerprints for different types of ligand bonding to an absorbing ion(6,7,14,15).

The X-ray absorption spectra of calcium-containing coals and reference compounds discussed in this paper were recorded at the Stanford Synchrotron Radiation Laboratory (SSRL) during a dedicated run of the Stanford Positron-Electron Acceleration Ring at an electron energy of 3.0 GeV. The calcium K-edge occurs at 4038 eV and data were collected from 3800 to 5000 eV, using a double Si (111) monochromator and a fluorescence detector similar to that of Stearn and Heald(16). A more detailed discussion of this work will appear elsewhere(17).

The samples examined were predominantly lignites from the Pust seam in Montana. However, data for two North Dakota lignites, for slagging and fouling deposits produced by those lignites, and for several subbituminous coals are also included.

Results and Discussion

Mossbauer spectroscopy results for all samples investigated are summarized in Table I. The percentages of the total sample iron contained in each of the iron-bearing minerals identified are given in columns 1 to 4, and the weight percentage of pyritic sulfur, determined from the pyrite absorption peak areas as discussed elsewhere(1), are given in column 5. It is seen that pyrite and minerals (iron sulfates and iron oxyhydroxide) that are probably derived from pyrite by weathering are the only iron-bearing species in these low-rank coals. Notably absent are contributions from iron-bearing clays and siderite which are common constituents of bituminous coals(1,2). Pyrite and iron oxyhydroxide are difficult to separate with room temperature Mossbauer spectroscopy(18). For example, in Figure 1 are shown the room temperature and 77 K spectra obtained from the Pust seam, C, lignite, which had been stored for several years prior to measurement. Although it is quite difficult to determine the relative amounts of pyrite and oxyhydroxide from the room temperature Mossbauer spectrum, the spectral contributions of the two phases are

readily resolved at 77 K.

CCSEM results for the approximate weight percentages of all inorganic phases are given in Table II. Perhaps the most interesting aspect of the CCSEM results for these low-rank coals as compared with similar data for bituminous coals is the abundance of Ca-rich phases. In most cases, these phases are not calcite, but are Ca-enriched macerals in which the Ca is uniformly dispersed throughout the coal, as illustrated by the SEM micrograph in Figure 2. The Ca-enriched macerals appear gray in this inverted backscattered electron image. An energy dispersive X-ray spectrum obtained from an individual maceral is shown on the right. As discussed below, EXAFS data indicate that this calcium is dispersed as salts of carboxylic acids.

The backscattered electron intensity of the Ca-enriched macerals is significantly smaller than that of calcite, and CCSEM can make a distinction, albeit somewhat imprecisely, between Ca-enriched macerals and calcite or other Ca-rich minerals on this basis. However, the CCSEM programs have not been properly calibrated to deal with the case of macerals enriched in an inorganic component such as Ca at this point. Consequently, the percentages indicated in Table II for the Ca-rich category are only a qualitative indication of the relative amounts of this species in the various low-rank coals examined. On the basis of the backscattered electron intensity, it appears that calcium is dispersed throughout the macerals of the lignites that have been examined, and is present partially in dispersed form and partially as calcite in the subbituminous coals. In fresh bituminous coals, calcium is present almost exclusively as calcite(3-5).

For comparison with Tables I and II, Table III gives the range and typical values of the mineral distributions observed in bituminous coals by the CCSEM and Mossbauer techniques, derived from studies of perhaps a hundred different bituminous coal samples in this laboratory. Some obvious differences in mineralogy are apparent. In addition to the difference in calcium dispersion and abundance already noted, it is seen that certain minerals common in bituminous coals, such as Fe-bearing clays (illite and chlorite) and siderite, are virtually absent in the low-rank samples of Tables I and II. Conversely, minerals such as barite ($BaSO_4$), apatite ($Ca_5(PO_4)_3OH$), and other Ca, Sr phosphates, are rather uncommon in bituminous coals.

EXAFS and XANES data for a Ca-rich sample of the Pust seam, A, lignite can be briefly summarized by reference to Figures 3 and 4. Figure 3 shows the XANES of the lignite, Ca acetate, and a fresh bituminious coal from the Pittsburgh seam rich in calcite. The strong similarity between the lignite and calcium acetate spectra is apparent. Similarly, a close similarity is also observed for the XANES of the fresh bituminous coal and that of a calcite standard. Examination of the XANES of several other standard compounds (CaO, $Ca(OH)_2$, and $CaSO_4 \cdot 2H_2O$) showed that none of these phases were present in detectable amounts in either coal. The strong similarity of the XANES of calcium acetate and that of the lignite is direct evidence that the calcium in this coal is associated with carboxyl groups in the macerals and is not contained in very fine (<0.1 μm) mineral matter.

Mathematical analysis of the EXAFS associated with the nearest-neighbor oxygen shell surrounding the Ca ions in the lignite was

accomplished using programs developed by Sandstrom(13). Briefly, the results indicate that the Ca is coordinated by six oxygens, possibly contributed in part by water molecules, at an average nearest neighbor distance of 2.39 Å. Additionally, the EXAFS data indicate that structural order at distances further from the Ca ions than the first coordination shell is essentially absent in the lignite, implying that the Ca sites are more or less randomly distributed throughout the macerals. This point is well illustrated by phase-shift subtracted Fourier transforms of the EXAFS data, which, as discussed elsewhere (12,13), should bear a reasonably close relationship to the radial distribution functions appropriate for the local environment of the Ca ions. In Figure 4, the magnitude of the phase-shift subtracted Fourier transform, $|F(r)|$, is shown for the lignite sample, calcium acetate, and a calcite-rich bituminous coal from the Pittsburgh seam. It is seen that the $|F(r)|$ curves for calcium acetate and the calcite-rich bituminous coal exhibit maxima corresponding not only to the nearest-neighbor oxygen shell, but also at the approximate locations of more distant calcium neighbor shells. The $|F(r)|$ curve of the lignite exhibits a clear maximum only at the oxygen nearest-neighbor shell distance. It is possible, however, that the small shoulder that appears on the high side of the oxygen shell peak in the lignite $|F(r)|$ curve (at approximately 3.5 Å) could correspond to the initial stages of Ca ion clustering.

Finally, it is noted that XANES and EXAFS spectra obtained from a severely weathered bituminous coal were nearly identical to those obtained from the lignite sample. This indicates that in the weathered coal calcium is also present in a dispersed form in which it is bonded to carboxyl groups in the macerals. A more detailed report of the Ca EXAFS investigation of lignite, fresh and weathered bituminous coal, and Ca reference compounds will appear elsewhere(17).

Analysis of Fouling and Slagging Deposits. It was observed that one of the two North Dakota lignites listed in Tables I and II produced heavy fouling deposits during combustion in a large utility furnace, while little or no difficulty was experienced in firing the other. As seen in Tables I and II, the inorganic phase distributions of these two coals are rather similar. Additionally, CCSEM and Mossbauer analysis of boiler-wall slag deposits produced by both coals gave rather similar results. A typical Mossbauer spectrum obtained from a boiler wall deposit (wall temperature ~1250°C) is shown in Figure 5, and a summary of the approximate phase distributions of the wall slag deposits produced by both coals is given in the inset. From the observed phases, it appears that the CaO-SiO_2-Fe_2O_3 phase diagram plays a key role in determining the slagging behavior of these coals. CCSEM analyses of fouling deposits produced by the two lignites are given in Table IV. It is seen that the only significant difference between the light and heavy deposits is the presence of an alkali sulfate mixture, containing Na, K, and Ca sulfates, in the latter. It is well known that alkali sulfates can react strongly with metal surfaces to produce alkali-iron sulfate mixtures that are partially molten over the temperature range from approximately 700 to 1100°C, causing severe fouling and corrosion problems(19).

Conclusions

In this paper, we have presented some examples of the usefulness of three techniques, Mossbauer spectroscopy, CCSEM, and EXAFS in the analysis of low-rank coals and combustion products of low-rank coals. Points of interest regarding the inorganic constituents of these coals include the high abundance of calcium bonded to carboxyl groups and dispersed throughout the macerals, the low abundance of illite, siderite, and calcite, and the presence of significant amounts of accessory minerals such as barite, apatite, and other phosphates. Areas that merit further investigation by these techniques include the analysis of fouling and slagging deposits, and structural studies of inorganic elements such as calcium that are dispersed through and bonded to the coal macerals.

Acknowledgments

The EXAFS experiments discussed in this paper were conducted in collaboration with F.W. Lytle and R.B. Greegor of the Boeing Company at the Stanford Synchrotron Radiation Laboratory, which is supported by the National Science Foundation and the Department of Energy.

References

1. Huffman, G.P., Huggins, F.E., Fuel, 1978, 57, 592-604.
2. Huggins, F.E., Huffman, G.P., Anal. Methods for Coal and Coal Products, Clarence Karr, Jr., Ed.; Academic: New York, 1979, Vol. 3, 371-423.
3. Huggins, F.E., Kosmack, D.A., Huffman, G.P., Lee, R.J., SEM/1980/I, 531-540, SEM Inc., AMF O'Hare (Chicago), IL (1980).
4. Huffman, G.P., Huggins, F.E., Lee, R.J., Proc. Int. Conference on Coal Science, Dusseldorf, 1981, 835-840, Verlag Glückauf GmbH, Essen, Germany (1981).
5. Huggins, F.E., Huffman, G.P., Lee, R.J., Coal and Coal Products: Analytical Characterization Techniques, E.L. Fuller, Jr., Ed.; ACS Symposium Series No. 205, 1982, 239-258, Amer. Chem. Soc., Washington, D.C.
6. Maylotte, D.H., Wong, J., St. Peters, R.L., Lytle, F.W., Greegor, R.B., Science, 1981, 214, 554.
7. Sandstrom, D.R., Filby, R.H., Lytle, F.W., Greegor, R.B., Fuel, 1982, 61, 195.
8. Hussain, Z., Barton, J.J., Umbach, E., Shirley, D.A., SSRL Activity Report, May 1981, A. Bienenstock and H. Winick, Eds.; p. VII-102.
9. Huffman, G.P., Huggins, F.E., Mossbauer Spectroscopy and Its Chemical Applications, J.G. Stevens and G.K. Shenoy, Eds.; Advances in Chemistry Series No. 194, 1981, 265-301, Amer. Chem. Soc., Washington, D.C.
10. Huffman, G.P., Huggins, F.E., Physics in the Steel Industry, F.C. Schwerer, Ed.; AIP Conf. Proc. No. 84, Amer. Inst. Physics, 1982, 149-201.

11. Lee, R.J., Kelly, J.F., SEM/1980/I, 303-310, SEM Inc., AMF O'Hare (Chicago), IL, (1980).
12. Lee, P.A., Citrin, P.H., Eisenberger, P., Kincaid, B.M., Rev. Mod. Phys., 1981, 53, 769.
13. Sandstrom, D.R., Proc. Workshop on EXAFS Analysis of Disordered Systems, Parma, Italy, 1981, to be published in Nuovo Cimento B.
14. Kutzler, F.W., Natoli, C.R., Misemer, D.K., Doniack, S., Hodgson, K.O., J. Chem. Phys., 1980, 73, 3274-88.
15. Bair, R.A., Goddard, W.A., Phys. Rev. B, 1980, 22, 2767-76.
16. Stearn, E.A., Heald, S., Rev. Sci. Instrum., 1979, 50, 1579.
17. Huggins, F.E., Huffman, G.P., Lytle, F.W., Greegor, R.B., "An EXAFS Investigation of Calcium in Coal," to be published in Proc. Int. Conference on Coal Science, Pittsburgh, 1983.
18. Huggins, F.E., Huffman, G.P., Kosmack, D.A., Lowenhaupt, D.E., Int. J. Coal Geology, 1980, 1, 75-81.
19. Reid, W.T., Chemistry of Coal Utilization, 1983, M.A. Elliot, Ed.; Suppl. Vol., Chapt. 21, 1389-1445, John Wiley & Sons, Inc.

TABLE I

Mossbauer Results For Low-Rank Coals

Sample	Percent of Total Iron Contained in: Pyrite	Jarosite	Ferrous Sulfate	Iron Oxy-hydroxide	Wt.% of Pyritic Sulfur
Pust seam, A-3	100	-	-	-	0.30
Pust seam, A-4	92	7	1	-	2.26
Pust seam, A-6	91	9	-	-	0.15
Pust seam, A-7	∿100+	-	-	-	∿0.03+
Pust seam, B-3	100	-	-	-	0.06
Pust seam, B-5	100	-	-	-	0.05
Pust seam, B-7	100	-	-	-	0.09
Pust seam, C	43	26	-	31	0.29
N.Dakota lignite, heavy fouling	91	6	2	-	0.50
N.Dakota lignite, light fouling	95	5	-	-	0.38
Rosebud subbituminous	65	16	19	-	0.15
Colstrip subbituminous	81	19	-	-	0.27

+Very weak spectrum; sample contained only 0.07% iron.

TABLE II

CCSEM Results for Low-Rank Coals (approximate weight percentages)

Sample	Quartz	Kaolinite	Mixed Silicates	Illite	Pyrite	Fe Sulfates	Fe-rich	Ca-rich+	Barite	Apatite	Other Phases Phase	Other Phases Percent
Pust seam, A-3	7	45	8	-	1	-	6	26	1	-	Montmorillonite	1
											Rutile	1
Pust seam, A-4	12	20	3	-	26	4	7	15	7	2	Fe-Ca-S	3
Pust seam, A-6	7	27	-	-	1	-	-	51	5	3	-	-
Pust seam, A-7	7	35	3	-	1	-	-	49	3	-	-	-
Pust seam, B-3	10	43	13	1	1	-	-	22	3	3	Montmorillonite	4
Pust Seam, B-5	14	38	3	-	1	-	-	38	5	-	Rutile	1
Pust seam, B-7	16	38	2	-	5	-	-	27	5	-	Ca-Fe-S	1
Pust seam, C	9	29	5	1	4	5	14	13	4	-	Ca-Fe	6
											Ca-Sr-Al-P*	4
											Jarosite	2
N.Dakota lighite, heavy fouling	24	13	20	3	19	1	1	14++	-	-	Montmorillonite	1
N.Dakota lignite, light fouling	28	16	13	2	10	-	2	23++	-	-	Montmorillonite	1
Rosebud, subbituminous	23	36	6	2	6	2	3	8	1	1	Ca-Sr-Al-P*	6
											Montmorillonite	1
											Rutile	1
Eveleth, subbituminous	18	23	22	12	4	-	3	7	-	1	Ca-Sr-Al-P*	8
Colstrip, subbituminous	22	25	6	3	8	-	3	29	-	-	Gypsum	4
Absaloka subbituminous	56	22	8	-	3	-	-	5	-	-	Rutile	3

+As discussed in the text, percentages given for the Ca-rich category are not quantitative.
*Minerals denoted by Ca-Sr-Al-P are probably crandallite $(Ca,Sr)Al_3(PO_4)_2(OH)_5H_2O$.
++Macerals enriched in Ca and S, with Ca/S ratios ∿1/1 to 6/1; some gypsum is probable.

TABLE III

Mineralogy of Bituminous Coals

CCSEM Analysis, Wt.% of Mineral Matter			Mossbauer Analysis, % of Total Sample Iron		
Mineral	Range	Typical	Mineral	Range	Typical
Quartz	5-44	18	Pyrite	25-100	62
Kaolinite	9-60	32	Ferrous Clay	0-56	18
Illite	2-29	14	Siderite/Ankerite	0-58	9
Chlorite	0-15	2	Ferrous Sulfate	0-18	3
Mixed Silicates	0-31	17	Jarosite	0-21	4
Pyrite	1-27	8	Wt.% Pyritic Sulfur*	0.08-1.51	0.35
Calcite/Dolomite	0-14	3			
Siderite/Ankerite	0-11	2			
Other	0-12	4			

*Determined by method of Ref. 1.

TABLE IV

CCSEM Results For Fouling Deposits, 800-1000°C

Species	Heavy (wt%)	Light (wt%)	
Al, Si-rich	5	5	
Quartz	3	8	
Hematite	2	3	
Ca-rich	10	7	
Mg-Ca	3	5	
Ca Ferrite	2	<1	
Ca-Si-Fe Glass	21	22	
Ca-Si + Glass	40	40	
Alkali Sulfate	2	0	
$CaSO_4$ + Alkali Sulfate	4	6	$CaSO_4$ only
Other	8	4	

Alkali Sulfate - Na/Ca/K = 1.0/0.5/0.1

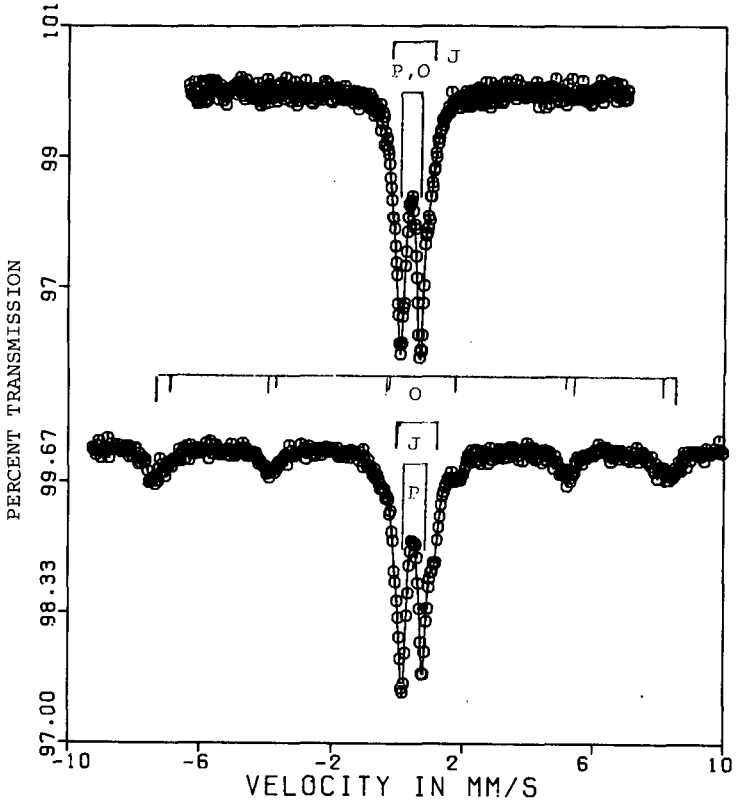

Fig. 1 Mossbauer spectra of the Pust seam, C, lignite. Pyrite (P), jarosite (J), and iron oxyhydroxide (O) are indicated.

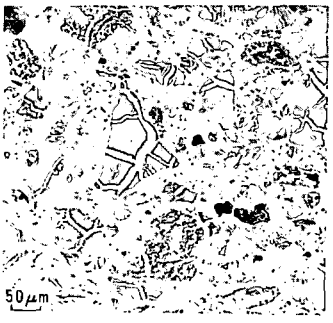

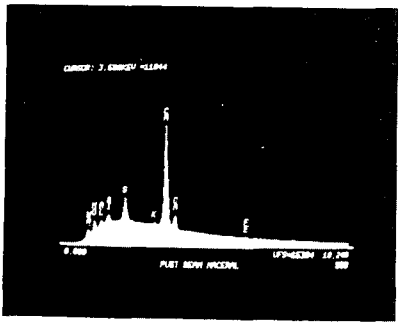

Fig. 2 **BACK-SCATTERED ELECTRON IMAGE** **ENERGY-DISPERSIVE X-RAY SPECTRUM**

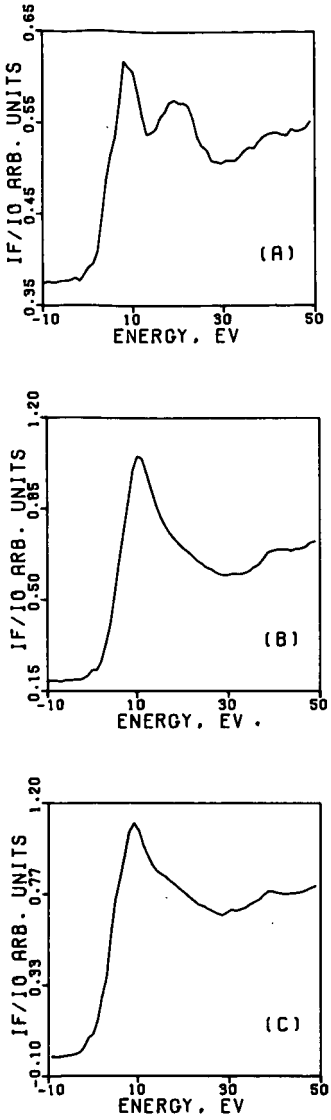

Fig. 3 XANES of: (A) calcite-rich bituminous coal; (B) the Pust seam lignite; (C) calcium acetate.

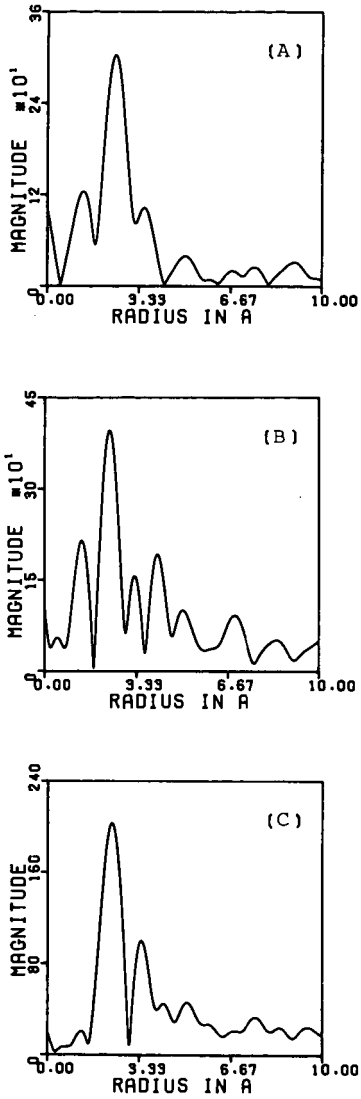

Fig. 4 Magnitudes of the phase-shift subtracted Fourier transform of: (A) the Pust seam lignite; (B) calcite-rich bituminous coal; (C) calcium acetate.

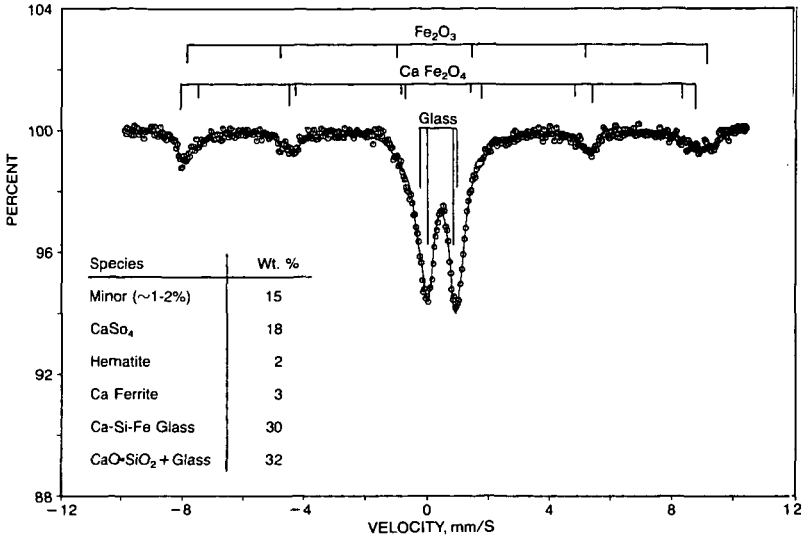

Fig. 5 Mossbauer spectrum of boiler-wall slag deposit. The approximate phase distribution determined from CCSEM and Mossbauer results is shown in the inset.